# New *Tetrahymena* basal body protein components identify basal body domain structure

Chandra L. Kilburn,[1] Chad G. Pearson,[1] Edwin P. Romijn,[2] Janet B. Meehl,[1] Thomas H. Giddings Jr.,[1] Brady P. Culver,[1] John R. Yates III,[2] and Mark Winey[1]

[1]Molecular, Cellular, and Developmental Biology, University of Colorado at Boulder, Boulder, CO 80309
[2]Department of Cell Biology, The Scripps Research Institute, La Jolla, CA 92037

Basal bodies organize the nine doublet microtubules found in cilia. Cilia are required for a variety of cellular functions, including motility and sensing stimuli. Understanding this biochemically complex organelle requires an inventory of the molecular components and the contribution each makes to the overall structure. We define a basal body proteome and determine the specific localization of basal body components in the ciliated protozoan *Tetrahymena thermophila*. Using a biochemical, bioinformatic, and genetic approach, we identify 97 known and candidate basal body proteins. 24 novel *T. thermophila* basal body proteins were identified, 19 of which were localized to the ultrastructural level, as seen by immunoelectron microscopy. Importantly, we find proteins from several structural domains within the basal body, allowing us to reveal how each component contributes to the overall organization. Thus, we present a high resolution localization map of basal body structure highlighting important new components for future functional studies.

## Introduction

Centrioles have dual roles in mammalian cells: as the core of the centrosome, they participate in forming the mitotic spindle, and, in quiescent cells, they migrate to the cell cortex to function as basal bodies for primary cilia formation. Like centrioles, basal bodies consist of a core structure (with peripheral components) of nine triplet microtubules organized into a cylinder. The cylinder can be further divided into distinct regions for which few of the molecular components or functions are known. Each domain fulfills a role for basal bodies and their attached cilia. These poorly defined functions include basal body assembly, basal body cortical attachment, protein recruitment for ciliary assembly, microtubule nucleation, and cellular polarity. Basal body defects lead to a range of diseases, including Bardet-Biedl syndrome and Polycystic Kidney Disease. An understanding of the basal body function and dysfunction in disease requires a comprehensive inventory of the proteins that comprise the basal body as well as the structural contribution of each. This is the first study to combine a basal body proteome with an ultrastructural analysis of newly identified basal body components. We reveal 24 new basal body proteins and describe the specific domains of localization for 19. Proteins were identified from various domains within the basal body, allowing us to predict their roles in basal body function.

C.L. Kilburn and C.G. Pearson contributed equally to this paper.

Correspondence to Mark Winey: mark.winey@colorado.edu

E.P. Romijn's present address is Philips Research, 5656AA Eindhoven, Netherlands.

Abbreviations used in this paper: HB, homogenization buffer; IB, isolation buffer; MudPIT, multidimensional protein identification technology; SPP, super proteose peptone.

The online version of this article contains supplemental material.

## Results and discussion

### Basal body protein isolation and identification

To describe a comprehensive inventory of the molecular components that comprise the *Tetrahymena thermophila* basal body, two separate isolation techniques were used in combination with the high throughput shotgun proteomic technique, multidimensional protein identification technology (MudPIT; Washburn et al., 2001). In one preparation, cell cortices (pellicles) with and without associated basal bodies were isolated to identify proteins dependent on γ-tubulin for basal body localization (Fig. 1 A; see Pellicle preparation section in Materials and methods). γ-Tubulin functions in microtubule nucleation and is involved in the early steps of basal body assembly (Shang et al., 2002). In *T. thermophila*, γ-tubulin is required for both the assembly and maintenance of basal bodies; transcriptional repression leads to the loss of basal bodies after 20 h (Shang et al., 2002). Pellicles were prepared from cells in the presence and


The Journal of Cell Biology, Vol. 178, No. 6, September 10, 2007 905–912
http://www.jcb.org/cgi/doi/10.1083/jcb.200703109

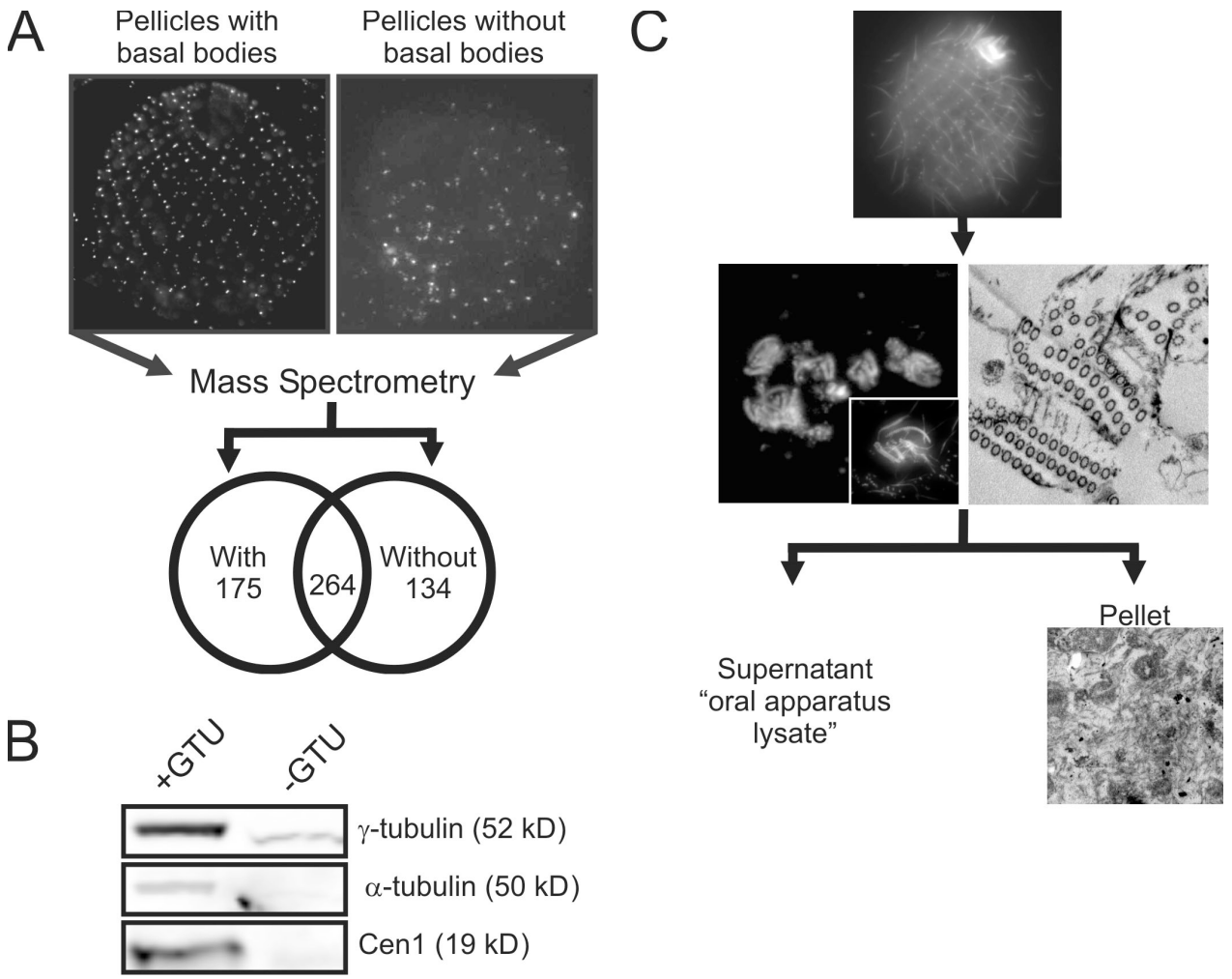


Figure 1. **Basal body protein preparations.** (A) Pellicles were made from cells expressing γ-tubulin (with basal bodies) and cells depleted of γ-tubulin (without basal bodies) for 24 h. An enrichment of basal bodies in the γ-tubulin–expressing cells was found by several methods. The loss of basal bodies was observed by decreased and mislocalized centrin staining in pellicles prepared from cells depleted of γ-tubulin compared with wild-type cells (top). At least a ninefold decrease in the number of basal bodies in γ-tubulin–depleted pellicles compared with pellicles expressing γ-tubulin was observed by electron microscopy (not depicted). Both samples were analyzed by mass spectrometry, and the proteins were tabulated. The Venn diagram describes the total number of proteins found by MudPIT analysis. All proteins identified in the sample lacking γ-tubulin were removed from the study. (B) Western blots of pellicles from cells with (+GTU) or without γ-tubulin (−GTU) show a decrease in three basal body proteins: γ-tubulin, α-tubulin, and centrin. Equal numbers of pellicles were loaded for each lane. (C) Basal body proteins were also prepared using isolated oral apparatuses. Oral apparatuses in whole cells and after biochemical isolation were visualized using GFP–α-tubulin. Basal bodies were prepared using modified methods (see Basal body lysate preparation section in Materials and methods; Wolfe, 1970). Isolated oral apparatuses are shown by fluorescence (left; inset of a single isolated oral apparatus) and electron microscopy (several rows of basal bodies are shown in cross section). Basal body proteins were extracted from the oral apparatus network producing the oral apparatus lysate. The electron micrograph of the extracted oral apparatuses (pellet) shows that basal bodies are no longer present; however, the underlying substructure of the oral apparatus remains. The final oral apparatus lysate was analyzed by MudPIT.

absence of γ-tubulin (Fig. 1, A and B). In the second preparation, the oral apparatuses were isolated from cells (Wolfe, 1970). The *T. thermophila* oral apparatus is composed of >100 ciliated and nonciliated basal bodies interconnected by a framework of microtubules and filaments to generate a feeding structure (Fig. 1 C; Wolfe, 1970). The associated basal bodies were extracted from the oral apparatus substructure (see Basal body lysate preparation section in Materials and methods). Basal body proteins extracted from the oral apparatus are reported to reassemble intermediate basal body assembly structures in vitro (Gavin, 1984). Using these two isolation techniques, we identified proteins necessary for intermediate structures in the basal body assembly pathway. Pellicle preparations allowed for the isolation of basal body components that are dependent on γ-tubulin for basal body localization, giving us insight into proteins involved in the maturation and maintenance of basal bodies. Proteins isolated from the oral apparatus allowed for the identification of components involved in the formation of the cartwheel, an early structure in basal body assembly (Dippell, 1968; Allen, 1969; Cavalier-Smith, 1974).

Proteins from all samples (pellicles with basal bodies, pellicles without basal bodies, and oral apparatuses) were identified using MudPIT (see Mass spectrometry section in Materials and methods). To identify proteins specifically found in the pellicle sample with basal bodies, components unique to each pellicle sample were tabulated (Fig. 1 A; Eng, 1994). Proteins identified

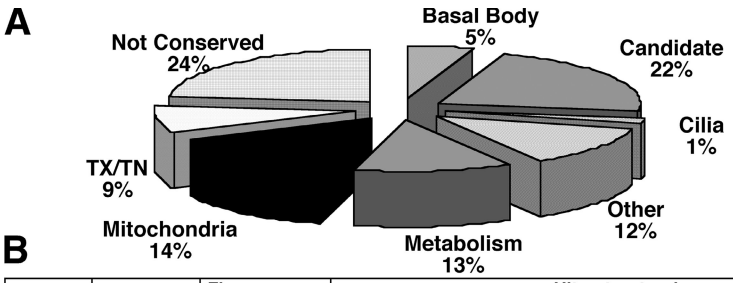


| Name | Domain | Fluorescence Localization | Ultrastructural Localization (*) |
|---|---|---|---|
| Cen1 | EF Hand | BB | Transition zone (22%), Site of assembly (34%), Midpoint (32%) |
| Bbc14 | None | BB | Site of assembly (69%) |
| Bbc20 | Lis1 | BB | Side of transition zone (93%) |
| Bbc23 | AhpC/TSA | BB, Cilia | Transition zone (20%), One side of MT scaffold (32%) |
| Bbc29 | Assemblin | BB, Cilia | Below cartwheel (87%) |
| Bbc30 | Prohibitin | BB | Collar (70%), MT scaffold (20%) |
| Bbc31 | DUF1042 | BB | Site of assembly (26%) |
| Bbc37 | EF Hand | BB, Cilia | NA |
| Bbc39 | Assemblin | BB | NA |
| Bbc42 | None | BB | NA |
| Bbc49 | None | BB | NA |
| Bbc52 | EF Hand | BB, Cilia | MT scaffold (41%), Transition zone (32%) |
| Bbc53 | HECT | BB, Cilia | Center of transition zone (33%), Distal end of collar (43%) |
| Bbc57 | None | BB, Cilia | MT scaffold (73%), Lumen (25%) |
| Bbc73 | EF Hand | BB, Cilia | MT scaffold (60%), Transition Zone (28%) |
| Bbc78 | Adh Short | BB | MT scaffold (83%) |
| Bbc82 | EF Hand | BB | Cartwheel (87%) |
| Bbc118 | EF Hand | BB, Cilia | NA |
| Eno1 | enolase | BB, Cilia | Collar (33%) |
| Ftt18 | 14-3-3 | BB | Collar (33%), Postciliary (33%) |
| Ftt49 | 14-3-3 | BB, Cilia | Collar (33%), Midpoint (50%) |
| PACRG | PACRG | BB, Cilia | Transition zone (54%), Collar (32%) |
| Poc1 | WD40 | BB | Site of assembly (45%), Cartwheel (39%) |
| Sas6a | PISA | BB | Center of cartwheel (100%) |
| Spag6 | ARM | BB, Cilia | Center of transition zone/docking site (63%) |

* Percent value corresponds to the percentage of gold particles that localize to the structural domain.

Figure 2. **24 new basal body proteins were identified by mass spectrometry.** (A) Based on BLAST analysis and gene ontology codes, proteins were classified into eight broad categories: (1) basal body, proteins known to associate with basal bodies/centrioles; (2) candidate, conserved proteins chosen as likely basal body candidates (BLAST e value $<10^{-6}$); (3) cilia, proteins known to associate with cilia; (4) other, a broad category of proteins involved in a variety of biological processes other than centriole function; (5) metabolism, proteins involved in metabolic processes; (6) mitochondria, proteins involved in mitochondrial function; (7) transcription/translation (TX/TN), proteins involved in RNA and protein production; and (8) not conserved, proteins with no vertebrate homologues (BLAST e value $>10^{-6}$). Detailed information for each protein is provided in Tables S1 and S2 (available at http://www.jcb.org/cgi/content/full/jcb.200703109/DC1). (B) Basal body components found and verified by live cell fluorescence imaging and immunoelectron microscopy. Protein name, domains, fluorescence localization, and ultrastructural localization are described. The percentages refer to the percentages of total gold particles localized to a specific domain by immunoelectron microscopy. The ultrastructural domains are illustrated in Fig. 3 D. BB, basal body; NA, no immunoelectron microscopy was performed; MT, microtubule.

from the sample lacking γ-tubulin and basal bodies were subtracted from the study. Of the 398 proteins that were removed, only one known basal body component (α-tubulin) was identified. α-Tubulin is a ubiquitous protein that is found throughout the *T. thermophila* cell cortex (Frankel, 2000), although it is greatly reduced from pellicles lacking γ-tubulin by Western blotting (Fig. 1 B).

### Basal body proteome

Combining the data from the two approaches yielded a basal body proteome of 355 proteins (Table S1, available at http://www.jcb.org/cgi/content/full/jcb.200703109/DC1); 175 proteins were dependent on γ-tubulin for association with the basal body, and 220 proteins were extracted from the isolated oral apparatuses. 40 proteins were present in both samples. All 355 proteins were annotated for (1) homologous proteins by BLAST searches in the *Homo sapiens*, *Drosophila melanogaster*, *Caenorhabditis elegans*, and *Paramecium tetraurelia* databases; (2) gene ontology codes; and (3) presence in proteomics studies of related structures (Table S2; Ostrowski et al., 2002; Andersen et al., 2003; Avidor-Reiss et al., 2004; Li et al., 2004; Liska et al., 2004; Keller et al., 2005; Pazour et al., 2005; Smith et al., 2005; Stolc et al., 2005; Broadhead et al., 2006). Based on these analyses, the proteins were classified into eight broad categories: basal body, candidate, cilia, other, metabolism, mitochondria, transcription/translation, and not conserved (Fig. 2 A). 22 of the 355 proteins (6%) were identified as known basal body/centriole components from previous studies (Table S1; Ostrowski et al., 2002; Andersen et al., 2003; Avidor-Reiss et al., 2004; Li et al., 2004; Keller et al., 2005; Pazour et al., 2005; Smith et al., 2005; Stolc et al., 2005). Approximately one third of the total proteins was classified as known or candidate basal body proteins, several of which were verified through this study. One third were likely contaminating proteins; another quarter were proteins that had no obvious homology to vertebrate cells (see Mass spectrometry section in Materials and methods). Because the centriole is a highly conserved organelle, the nonconserved proteins were not studied further. However, it is worth noting that these proteins may be important for future studies in understanding *T. thermophila* basal body duplication and assembly. By analogy, Bld10p, which is found in *Chlamydomonas reinhardtii*, is involved in the early assembly steps of the basal body; however, an obvious Bld10 candidate has not been found in other species (Matsuura et al., 2004).

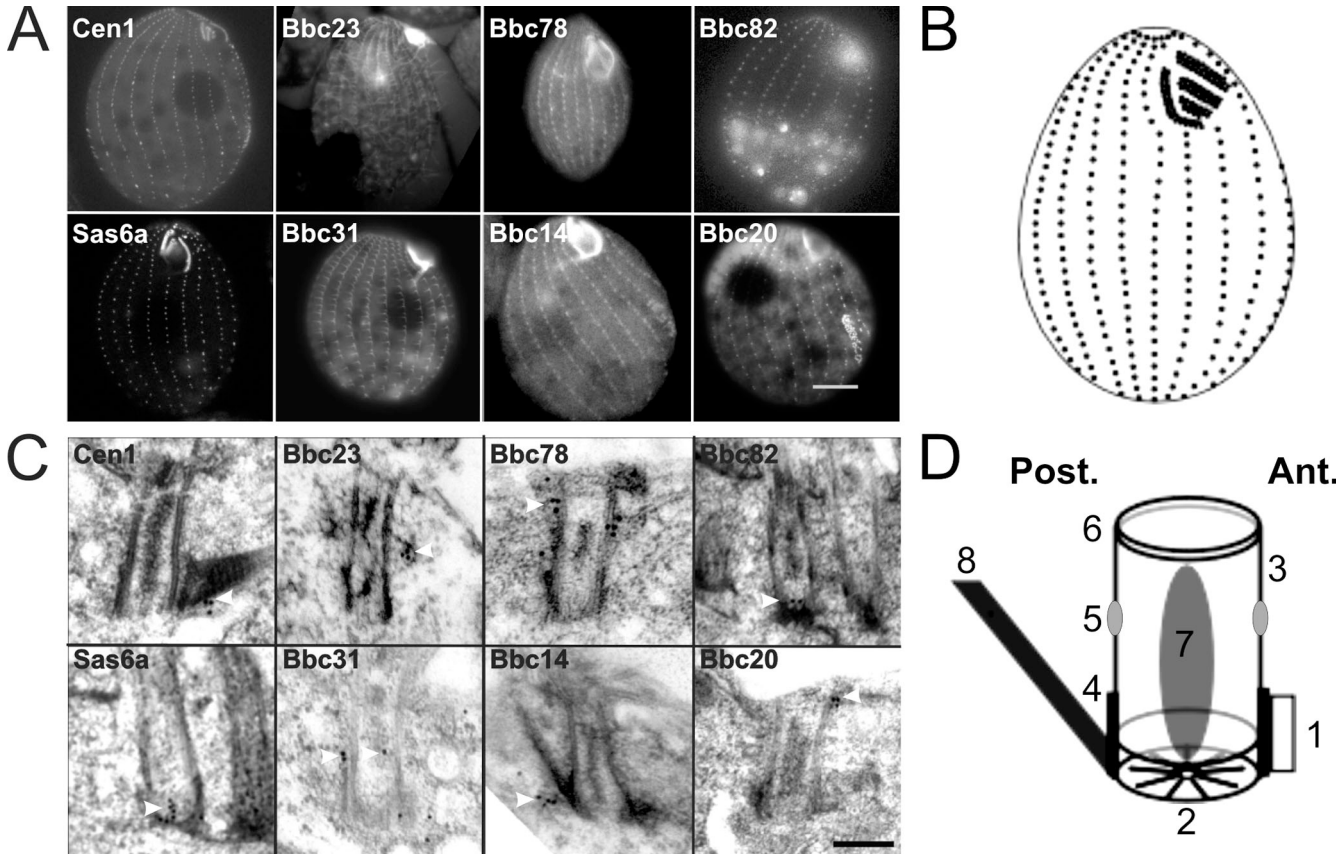


Figure 3. **Localization of selected basal body components.** (A) Live cell images of GFP-tagged Cen1, Bbc23, Bbc78, Bbc82, Sas6a, Bbc31, Bbc14, and Bbc20. Cen1, a known basal body component and a proteomics hit, is shown as a control. (B) Schematic of the organization of basal bodies in a *T. thermophila* cell. Basal bodies are found in cortical rows and at the oral apparatus. (C) Immunoelectron microscopy of longitudinal basal body sections from cells expressing GFP fusion proteins: Cen1, Bbc23, Bbc78, Bbc82, Sas-6a, Bbc31, Bbc14, and Bbc20. Cells were indirectly labeled with anti-GFP antibodies and gold-conjugated secondary antibodies. Locations of the gold particles are highlighted with arrowheads. (D) Schematic of the organization of a basal body. The structural domains shown are the (1) site of nascent basal body assembly, (2) cartwheel, (3) microtubule scaffold, (4) collar, (5) midpoint, (6) transition zone, (7) lumen, and (8) postciliary microtubules. The posterior and the anterior sides of the basal body in reference to the cell geometry are indicated. Bars (A), 10 μm; (C) 200 nm.

We classified 79 proteins as centriole/basal body candidates because they fell into at least one or more of the following three categories. First, proteins were chosen that contained domains or structural motifs that were previously found to associate with basal bodies, centrioles, or microtubules. These included domains that interact with microtubule structures (e.g., assemblin, glyceraldehyde-3-phosphate dehydrogenase, Lis2, and EF hand) or domains found in many known centriole/centrosome proteins (e.g., WD40 repeats, HEAT repeats, DM10, 14-3-3 domains, or coiled-coil domains). Second, proteins were classified as candidates if homologues were identified by previous studies using proteomic, bioinformatic, or comparative genomic approaches in a variety of organisms, including *T. thermophila*, *C. reinhardtii*, *Trypanosoma brucei*, *Drosophila*, and human cells, to identify molecular components of centrioles (Keller et al., 2005), centrosomes (Andersen et al., 2003), or cilia (Ostrowski et al., 2002; Avidor-Reiss et al., 2004; Li et al., 2004; Pazour et al., 2005; Smith et al., 2005; Stolc et al., 2005). Many proteins were identified in multiple studies, confirming that not only is the structure and function of microtubule-organizing centers conserved across phylogeny but the molecular components are conserved as well (Table S2). This comparative proteomics approach enabled cross validation of proteins to make them stronger candidate basal body components. Proteins identified through this approach include 17 of the POC (proteome of centriole) and BUG (basal body proteins with upregulated genes) proteins found in the first reported proteomic analysis of centrioles (Keller et al., 2005). Although each of the aforementioned studies identified new potential protein components of the studied structure, localization studies are necessary to confirm the identity as a basal body/centriole component. Finally, we focused on proteins in which mutations in the human orthologues are known to cause ciliary dysfunction and disease. For example, mutations in LIS-1 cause mental retardation, neurodegeneration, and male sterility (Faulkner et al., 2000; Smith et al., 2000), mutations in Spag-6 cause hydrocephalus (Sapiro et al., 2002), and mutations in Parkin coregulated gene (PACRG) result in sterility (Lorenzetti et al., 2004). *T. thermophila* orthologues for each of these proteins were identified.

### Fluorescence localization of basal body proteins

Proteins classified as candidates through the aforementioned secondary screen were then selected for biological validation by GFP fluorescence localization in live *T. thermophila* cells.

We generated GFP fusions to 40 genes, all of which were expressed (not depicted), and 24 of the proteins localized to basal bodies (summarized in Fig. 2 B; also see Figs. S1–3; available at http://www.jcb.org/cgi/content/full/jcb.200703109/DC1). This is in contrast to the diffuse localization of GFP alone (Fig. S1). We used *T. thermophila* centrin (Cen1), a known basal body component and proteomic hit found in our study, as a positive control for proper basal body localization (Stemm-Wolf et al., 2005). Each new basal body component localized in the canonical basal body pattern for both cortical rows and the oral apparatus (Fig. 3, A and B; and Fig. S1–3). In addition, *T. thermophila* have 17 microtubule-containing structures in the cell (Gaertig, 2000) and several proteins localized to multiple microtubular structures. For example, we identified proteins that localize to the micronuclear spindle (e.g., Bbc23) and cilia (e.g., Spag-6) in addition to basal bodies. Of the 24 newly confirmed basal body components, all but one (BBC14) are conserved in most of the eukaryotes examined.

### High resolution localization of basal body proteins

To begin to understand the function of each newly identified basal body component, we determined the ultrastructural localization using immunoelectron microscopy (see Immunoelectron microscopy section in Materials and methods). Detailed localization data provide critical clues for function, and this is the first study describing protein localization to basal body domains in combination with a basal body proteome. Basal bodies consist of a highly conserved structure built on a core of nine symmetrically arrayed triplet microtubules with peripheral components necessary for microtubule nucleation, basal body anchoring to the plasma membrane, polarity establishment, and protein docking. Distinct regions exist for which few functions are known (Fig. 3 D). Assembly of the nascent organelle in ciliates reveals several intermediate structures in basal body formation (Dippell, 1968; Allen, 1969; Cavalier-Smith, 1974). Localization of a component to an intermediate structure implies not only a role at a given stage in assembly but also information about the role the protein plays in basal body function. In this study, we define the localization of 19 newly identified basal body components to intermediate structures found in the assembly pathway and to mature basal bodies.

Basal body assembly begins with the appearance of an amorphous disk structure near the base or proximal end of the existing mother basal body. Bbc14, Bbc31, and Poc1 localized to this site of assembly, as does centrin (Fig. 3 C; Salisbury et al., 1984; Guerra et al., 2003; Stemm-Wolf et al., 2005). The cartwheel, which consists of a central hub and nine radial spokes, assembles on top of the amorphous disk. Three proteins (Poc1, Bbc82, and Sas6a) localize to the cartwheel of mature basal bodies, a domain also observed early in assembly (Figs. 3 C, S2, and S3). The *C. reinhardtii* Bld10 protein also localizes to cartwheels and is essential for basal body assembly (Matsuura et al., 2004). In addition, Bbc29 localized to the proximal end of the cartwheel (Fig. S1). Thus, Bbc29, Poc1, Bbc82, and Sas6a may all be crucial for early basal body assembly and/or maintenance.

At the tip of each spoke of the cartwheel, the A and subsequently the B and C microtubules are nucleated perpendicular to the mother basal body. These microtubules form the triplet blades for the cylindrical structure of the probasal body. During probasal body maturation, the cylinder elongates and separates from the mother as it inserts into the membrane, forming a structure that will nucleate a cilium. The mature and functional basal body exhibits several distinct morphological domains for which we identified new proteins localizing to each (Figs. 2 B and 3 D).

Bbc23, Bbc30, Bbc52, Bbc57, Bbc73, and Bbc78 localized to the microtubule scaffold or walls of the core cylinder (Figs. 3 C, S1, and S2). These proteins appeared as a sheath surrounding the core structure. Similarly, ε-tubulin (Dupuis-Williams et al., 2002; Dutcher et al., 2002) and *T. thermophila* actin (Hoey and Gavin, 1992) are found surrounding the basal body cylinder. Although ε-tubulin appears to have a conserved role in assembling or maintaining the triplet microtubule structure, actin contributes to normal ciliary structure and motility (Williams et al., 2006).

In addition to the general localization of proteins along the length of the basal body cylinder, regions of discrete localization were also observed. The proximal one third of the microtubule scaffold is surrounded by an electron-dense collar structure. Six proteins (Bbc30, Bbc53, Eno1, Ftt18, Ftt49, and PACRG) localized to the collar (Fig. 3 C and Figs. S1–3). The collar is used as a site of attachment for cortical structures that contribute to the highly organized cytoskeleton of the *T. thermophila* cell (Frankel, 2000). Finally, Cen1 and Ftt49 localized to a common site approximately equidistant from the ends of the basal body. This domain was defined as the midpoint and may be analogous to satellite structures found in centrioles.

The distal-most region of the mature basal body is the transition zone, which appears as two sheets in longitudinal sections (Marshall and Nonaka, 2006). Proteins localizing to the transition zone play roles in creating a foundation for the nucleation of ciliary microtubules and/or as a docking site for protein transport. Bbc20, Bbc23, Bbc52, Bbc53, Bbc73, PACRG, and Spag6 localized to the transition zone (Fig. 3 C and Figs. S1–3). Specifically, Bbc53 and Spag6 localized to the center of the transition zone at the site of central pair assembly. This localization is consistent with the role of Spag6 in the assembly and/or maintenance of ciliary central pair microtubules (Sapiro et al., 2002), whereas Bbc20 (a Lisencephaly-1 domain–containing protein) localized to the side of the transition zone similar to intraflagellar transport protein localization at basal bodies (Cole et al., 1998). It should be noted that this localization is distinct from the transition fiber localization observed for IFT52 (Deane et al., 2001), although both regions seem to function in intraflagellar transport motility. Mutations in Lis-1 domain proteins cause several pathologies in humans, including mental retardation and neurodegeneration.

The mature basal body lumen is filled with an opaque material extending from the cartwheel nearly to the terminal plate. To our knowledge, only centrin and γ-tubulin have been localized to this region and are thought to form a continuous filament scaffold throughout the lumen (Fuller et al., 1995; Geimer and Melkonian, 2005). We have identified one additional luminal basal body component, Bbc57.

The ultrastructural localization of new basal body proteins is illustrated in a compilation model describing the molecular

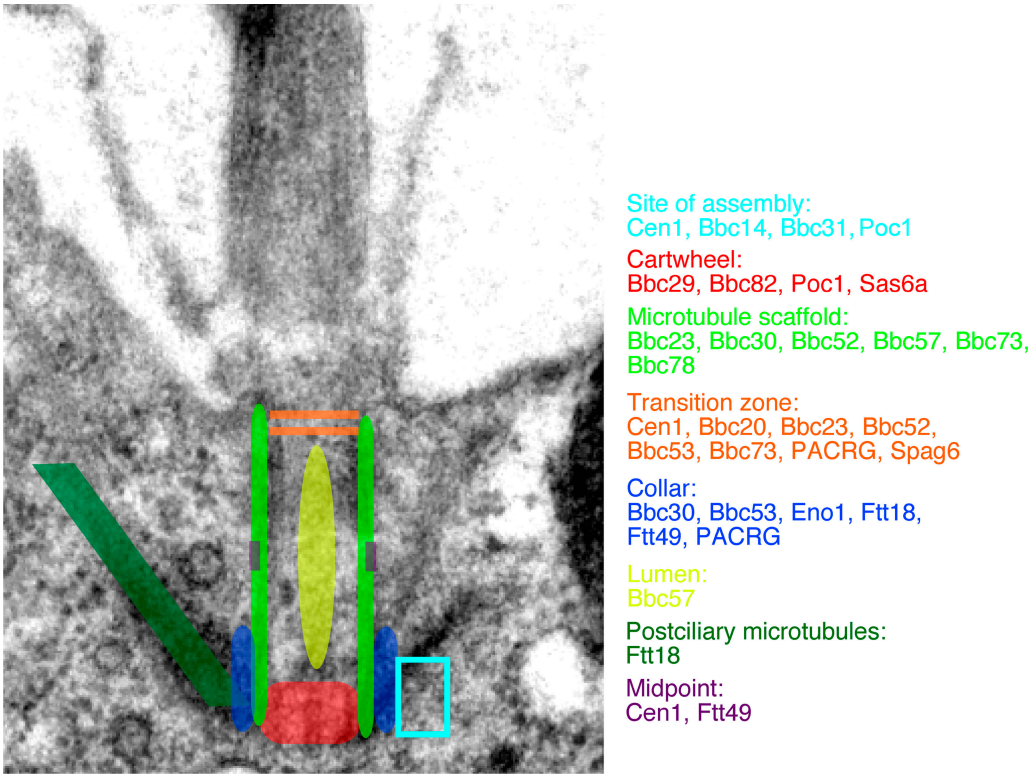


Figure 4. **New *T. thermophila* basal body components were shown to localize to discrete structural domains.** Protein localizations were assigned to specific domains if at least 20% of all gold particles in the immunoelectron microscopy compilation images are associated with the region. New protein components are listed in Fig. 2 B and in Figs. S1–3 (available at http://www.jcb.org/cgi/content/full/jcb.200703109/DC1). Color reference and domain are listed for each new basal body component described.

architecture of the organelle (Fig. 4). By localizing basal body components into specific domains, we can begin to consider distinct functional roles for these proteins as well as possible interacting proteins. We have identified 24 new basal body protein components and have defined a high resolution map for 19. These data provide a detailed, albeit preliminary, molecular view of the basal body structure. Similar structural, biochemical, and genetic studies have contributed to the comprehensive picture of the yeast spindle pole body (for review see Jaspersen and Winey, 2004), nuclear pore complexes (Rout et al., 2000), and kinetochores (Westermann et al., 2007). A comprehensive understanding of basal body and centriole function throughout the cell cycle requires an inventory of the components and how each contributes to the overall structure. Our proteomic and molecular approach combined with future genetic and biochemical studies will provide a comprehensive molecular map for understanding the assembly and functions of basal bodies and centrioles.

## Materials and methods

### Strains and culture conditions

*T. thermophila* strains CU428, SB1969, B2086 (*Tetrahymena* Stock Center, Cornell University), and TTMGII (a gift from M. Gorovsky, University of Rochester, Rochester, NY) were used in this study. Unless specified, cells were grown in super proteose peptone (SPP) media (2% proteose peptone, 0.1% yeast extract, 0.2% glucose, and 0.003% Fe-EDTA) at 30°C. TTMGII cells were grown in SPP with 1% proteose peptone at 22°C. For conjugation, midlog phase cells were washed and resuspended in starvation media (10 mM Tris, pH 7.5). After 18–20 h, equal numbers of each mating type were combined and incubated at 30°C.

### γ-Tubulin shutoff

TTMGII (Shang et al., 2002) cells were grown to midlog phase in SPP with 1 mg/ml $CdCl_2$ to maintain γ-tubulin expression. To deplete γ-tubulin, cells were washed three times in starvation media and diluted to $3 \times 10^3$ cells/ml without $CdCl_2$ for 24 h at 22°C before pellicle preparation.

### Pellicle preparation

Pellicles were prepared from 1 liter of TTMGII cells grown to $\sim 2 \times 10^5$ cells/ml in SPP with and without 1 mg/ml $CdCl_2$. Cells were spun for 15 min at 600 *g* and 4°C and were resuspended in 15 ml of ice-cold homogenization buffer (HB; 20 mM Hepes, pH 7.0, 40 mM NaCl, 0.3 M sucrose, and 2 mM $MgCl_2$) plus protease inhibitors (1 μg/ml leupeptin, 15 μg/ml E64, 10 μg/ml chymostatin, and 10 μg/ml antipain). Cells were spun again for 1 min, resuspended in 15 ml HB, left on ice for 10 min, transferred to a Dounce homogenizer, and lysed with 40 strokes. The lysed cells were loaded onto a sucrose step gradient (1.46 and 1 M sucrose) and spun at 2,500 rpm for 10 min at 4°C. Pellicles were collected from the interphase layer and washed with HB (the protocol was adapted from Nozawa and Thompson [1971]). Electron micrographs show that much of the cytoplasm and contaminating organelles were removed through this preparation. Pellicles were solubilized in HB + 1% NP-40 and TCA precipitated.

### Basal body lysate preparation

Basal body protein lysates were prepared using modified methods that were previously published (Wolfe, 1970). 1.5 liters of cells were grown to $\sim 3 \times 10^5$ cells/ml in SPP, harvested, and washed with cold 0.12 M sucrose. All of the following procedures were performed at 4°C. Cells were incubated in isolation buffer (IB; 1 M sucrose, 1 mM EDTA, 0.1% 2-mercaptoethanol, 10 mM Tris, pH 7.3, at room temperature, and 0.75% Triton X-100) for 4 h to isolate oral apparatuses from the cell cortex. Samples were then washed with 2% Triton X-100 in IB before douncing in a 50-ml tissue homogenizer. Samples were washed again with 2% Triton X-100 in IB, filtered through an 8.0-μm polycarbonate filter (Nucleopore Filter Corp.), and spun, and the isolated oral apparatuses were resuspended in IB without detergent (Fig. 1 C). To isolate basal body proteins (basal body lysate) from the oral apparatus framework, KCl was added to a final concentration of

1 M and incubated for 18 h with gentle stirring. Samples were then spun at 30,000 *g* for 30 min to pellet the oral apparatus framework, leaving the soluble basal body lysate. The lysate was then dialyzed into storage buffer (10 mM MES, pH 6.7, 150 mM KCl, 0.5 mM $MgSO_4$, 1 mM EGTA, 0.5 mM DTT, and 1 M sucrose) and TCA precipitated.

**Mass spectrometry**

TCA precipitates from purified basal bodies were resuspended in 200 mM $Na_2CO_3$, pH 11, adjusted to 8 M urea, reduced, and alkylated as reported previously (Washburn et al., 2001). 5 μg proteinase K was added to the sample and incubated at 37°C for 5 h in a Thermomixer (Brinkmann; Wu et al., 2003). The digestion was stopped by the addition of formic acid to 5%, microcentrifuged at 18,000 *g* and 4°C for 15 min to remove particulates, and subsequently pressure loaded on a 6-cm-long fritted (Meiring, 2002) microcapillary-fused silica column (250-μm inner diameter) packed with 3 cm/5 μm C-18 resin (Aqua; Phenomenex) and 3 cm/5 μm strong cation exchange resin (Whatman). This precolumn was coupled via a true zero dead volume union (UpChurch Scientific) to a 15-cm/75-μm analytical column packed with 3 μm C-18 resin (Aqua; Phenomenex). Liquid chromatography/liquid chromatography/mass spectrometry/mass spectrometry was then performed as described previously (Keller et al., 2005). Next, the collection of resulting ms2 spectra was searched against the preliminary sequence data for *T. thermophila* using the SEQUEST algorithm (Eng, 1994). Data for *T. thermophila* scaffolds was obtained from The Institute for Genomic Research (TIGR; http://www.ciliate.org; Eisen et al., 2006). Peptide identifications were organized and filtered using the DTASelect and Contrast programs (Tabb et al., 2002). Filtering criteria for positive protein identifications for all purifications were the identification of two unique peptides with a false positive rate ≤5%. The proteins corresponding to the matching peptides are listed in Table S1 along with the number of peptides matched to each protein and spectral count, which gives an indication of the relative abundance of the protein in the sample. All proteins were analyzed with BLAST searches to human, *Drosophila*, *P. tetraurelia*, *C. reinhardtii*, and *C. elegans* databases (BLAST e value $> 10^{-6}$).

**Western blotting**

To demonstrate the presence of γ-tubulin, α-tubulin, and centrin in pellicles, $0.5 \times 10^5$ pellicles (solubilized in SDS-PAGE buffer) per lane were separated by SDS-PAGE. Blots were performed with anti–γ-tubulin antibody (GTU88; 1:500), anticentrin (1:1,000), or anti–α-tubulin (DM1A; 1:500). Proteins were detected using an infrared scanner (Odyssey System; LI-COR).

**Plasmid construction and protein expression**

Candidate gene ORFs (preliminary gene predictions TIGR Genome Database) were amplified from genomic DNA by PCR with attached cloning sites. The products were cloned into pIGF.1 (gift from D. Chalker, Washington University, St. Louis, MO) to generate an N-terminal GFP fusion under the control of the metallothionein promoter. Protein expression was induced by the addition of 0.2–1.0 μg/ml $CdCl_2$ for 1–2 h, and cells were then washed into fresh media without induction for 2–4 h. Live cells were washed in 10 mM Tris, pH 7.4, and GFP was imaged using an upright microscope (DMRXA/RF4/V; Leica) with a CCD camera (SensiCam; Cooke) at 25°C. Images were collected using a PL-APO 63× NA 1.32 objective (Leica) and the Slidebook software package (version 3.0.6.6; Intelligent Imaging Innovations). Through z series, maximum projections were generated using ImageJ software (National Institutes of Health [NIH]).

**Immunoelectron microscopy**

*T. thermophila* cells were pelleted, high-pressure frozen in a machine (HPM-010; Bal-Tec), freeze substituted in 0.25% glutaraldehyde/0.1% uranyl acetate in acetone, and embedded in Lowicryl HM20. 60-nm serial sections were cut and put on nickel slot grids, blocked with 1% milk in PBS–Tween 20, and incubated with anti-GFP (a gift from J. Kahana and P. Silver, Dana Farber Cancer Institute, Boston, MA) at 1:100. 15 nm gold-conjugated secondary antibody was applied to the grids at a dilution of 1:20 (Ted Pella). Grids were poststained with 2% uranyl acetate and lead citrate. Images were collected using an electron microscope (CM10; Philips) equipped with a digital camera (BioScan2; Gatan) and digital micrograph software (Gatan). The domains of localization for each protein were determined by imaging the basal bodies of at least five cells and compiling the gold particles onto one schematic cartoon image (Figs. S1–3). Domain localization was defined if at least 20% of the total gold particles were seen at a specific region.

**Online supplemental material**

Figs. S1–3 describe the fluorescence and immunoelectron microscopy localization of basal body components found in this study. Table S1 shows a summary of the mass spectrometry data. Table S2 shows a summary of the comparison to other proteomics/genomics studies. Online supplemental material is available at http://www.jcb.org/cgi/content/full/jcb.200703109/DC1.

We thank A. Sitikov and A. Turkewitz for their adaptation of the Nozawa and Thompson pellicle protocol. We thank Drs. Marty Gorovsky, Doug Chalker, Aaron Turkewitz, and Eric Cole for strains, vectors, and helpful discussions. We thank Alex Stemm-Wolf for helpful advice and discussions. We thank Dr. Jason Stumpff for critical reading of the manuscript.

C.L. Kilburn was supported by the Signaling and Cellular Regulation Training grant from the NIH (T32 GM008759). C.G. Pearson was supported by the Damon Runyon Cancer Research Foundation (grant 1879-05). This work was supported by a grant from the NIH (GM074746) to M. Winey. J.R. Yates acknowledges support from the NIH (grant P41 RR11823).

Submitted: 19 March 2007
Accepted: 15 July 2007

## References

Allen, R.D. 1969. The morphogenesis of basal bodies and accessory structures of the cortex of the ciliated protozoan *Tetrahymena pyriformis*. *J. Cell Biol.* 40:716–733.

Andersen, J.S., C.J. Wilkinson, T. Mayor, P. Mortensen, E.A. Nigg, and M. Mann. 2003. Proteomic characterization of the human centrosome by protein correlation profiling. *Nature*. 426:570–574.

Avidor-Reiss, T., A.M. Maer, E. Koundakjian, A. Polyanovsky, T. Keil, S. Subramaniam, and C.S. Zuker. 2004. Decoding cilia function: defining specialized genes required for compartmentalized cilia biogenesis. *Cell*. 117:527–539.

Broadhead, R., H.R. Dawe, H. Farr, S. Griffiths, S.R. Hart, N. Portman, M.K. Shaw, M.L. Ginger, S.J. Gaskell, P.G. McKean, and K. Gull. 2006. Flagellar motility is required for the viability of the bloodstream trypanosome. *Nature*. 440:224–227.

Cavalier-Smith, T. 1974. Basal body and flagellar development during the vegetative cell cycle and the sexual cycle of *Chlamydomonas reinhardii*. *J. Cell Sci.* 16:529–556.

Cole, D.G., D.R. Diener, A.L. Himelblau, P.L. Beech, J.C. Fuster, and J.L. Rosenbaum. 1998. *Chlamydomonas* kinesin-II-dependent intraflagellar transport (IFT): IFT particles contain proteins required for ciliary assembly in *Caenorhabditis elegans* sensory neurons. *J. Cell Biol.* 141:993–1008.

Deane, J.A., D.G. Cole, E.S. Seeley, D.R. Diener, and J.L. Rosenbaum. 2001. Localization of intraflagellar transport protein IFT52 identifies basal body transitional fibers as the docking site for IFT particles. *Curr. Biol.* 11:1586–1590.

Dippell, R.V. 1968. The development of basal bodies in *Paramecium*. *Proc. Natl. Acad. Sci. USA*. 61:461–468.

Dupuis-Williams, P., A. Fleury-Aubusson, N.G. de Loubresse, H. Geoffroy, L. Vayssie, A. Galvani, A. Espigat, and J. Rossier. 2002. Functional role of epsilon-tubulin in the assembly of the centriolar microtubule scaffold. *J. Cell Biol.* 158:1183–1193.

Dutcher, S.K., N.S. Morrissette, A.M. Preble, C. Rackley, and J. Stanga. 2002. Epsilon-tubulin is an essential component of the centriole. *Mol. Biol. Cell*. 13:3859–3869.

Eisen, J.A., R.S. Coyne, M. Wu, D. Wu, M. Thiagarajan, J.R. Wortman, J.H. Badger, Q. Ren, P. Amedeo, K.M. Jones, et al. 2006. Macronuclear genome sequence of the ciliate *Tetrahymena thermophila*, a model eukaryote. *PLoS Biol.* 4:e286.

Eng, J.K., A.L. McCormack, and J.R. Yates. 1994. An approach to correlate tandem mass spectral data of peptides with amino acid sequences in a protein database. *J. Am. Soc. Mass. Spectrom.* 5:976–989.

Faulkner, N.E., D.L. Dujardin, C.Y. Tai, K.T. Vaughan, C.B. O'Connell, Y. Wang, and R.B. Vallee. 2000. A role for the lissencephaly gene *LIS1* in mitosis and cytoplasmic dynein function. *Nat. Cell Biol.* 2:784–791.

Frankel, J. 2000. Cell biology of *Tetrahymena thermophila*. *Methods Cell Biol.* 62:27–125.

Fuller, S.D., B.E. Gowen, S. Reinsch, A. Sawyer, B. Buendia, R. Wepf, and E. Karsenti. 1995. The core of the mammalian centriole contains gamma-tubulin. *Curr. Biol.* 5:1384–1393.

Gaertig, J. 2000. Molecular mechanisms of microtubular organelle assembly in *Tetrahymena*. *J. Eukaryot. Microbiol.* 47:185–190.

Gavin, R.H. 1984. In vitro reassembly of basal body components. *J. Cell Sci.* 66:147–154.

Geimer, S., and M. Melkonian. 2005. Centrin scaffold in *Chlamydomonas reinhardtii* revealed by immunoelectron microscopy. *Eukaryot. Cell*. 4:1253–1263.

Guerra, C., Y. Wada, V. Leick, A. Bell, and P. Satir. 2003. Cloning, localization, and axonemal function of *Tetrahymena* centrin. *Mol. Biol. Cell*. 14:251–261.

Hoey, J.G., and R.H. Gavin. 1992. Localization of actin in the *Tetrahymena* basal body-cage complex. *J. Cell Sci.* 103:629–641.

Jaspersen, S.L., and M. Winey. 2004. The budding yeast spindle pole body: structure, duplication, and function. *Annu. Rev. Cell Dev. Biol.* 20:1–28.

Keller, L.C., E.P. Romijn, I. Zamora, J.R. Yates III, and W.F. Marshall. 2005. Proteomic analysis of isolated *Chlamydomonas* centrioles reveals orthologs of ciliary-disease genes. *Curr. Biol.* 15:1090–1098.

Li, J.B., J.M. Gerdes, C.J. Haycraft, Y. Fan, T.M. Teslovich, H. May-Simera, H. Li, O.E. Blacque, L. Li, C.C. Leitch, et al. 2004. Comparative genomics identifies a flagellar and basal body proteome that includes the *BBS5* human disease gene. *Cell*. 117:541–552.

Liska, A.J., A.V. Popov, S. Sunyaev, P. Coughlin, B. Habermann, A. Shevchenko, P. Bork, E. Karsenti, and A. Shevchenko. 2004. Homology-based functional proteomics by mass spectrometry: application to the *Xenopus* microtubule-associated proteome. *Proteomics*. 4:2707–2721.

Lorenzetti, D., C.E. Bishop, and M.J. Justice. 2004. Deletion of the Parkin coregulated gene causes male sterility in the quaking(viable) mouse mutant. *Proc. Natl. Acad. Sci. USA*. 101:8402–8407.

Marshall, W.F., and S. Nonaka. 2006. Cilia: tuning in to the cell's antenna. *Curr. Biol.* 16:R604–R614.

Matsuura, K., P.A. Lefebvre, R. Kamiya, and M. Hirono. 2004. Bld10p, a novel protein essential for basal body assembly in *Chlamydomonas*: localization to the cartwheel, the first ninefold symmetrical structure appearing during assembly. *J. Cell Biol.* 165:663–671.

Meiring, H.D., E. van der Heeft, G.J. ten Hove, and A.P. de Jong. 2002. Nanoscale LC-MS(n): technical design and applications to peptide and protein analysis. *J. Sep. Sci*. 25:557–568.

Nozawa, Y., and G.A. Thompson Jr. 1971. Studies of membrane formation in *Tetrahymena pyriformis*. II. Isolation and lipid analysis of cell fractions. *J. Cell Biol.* 49:712–721.

Ostrowski, L.E., K. Blackburn, K.M. Radde, M.B. Moyer, D.M. Schlatzer, A. Moseley, and R.C. Boucher. 2002. A proteomic analysis of human cilia: identification of novel components. *Mol. Cell. Proteomics*. 1:451–465.

Pazour, G.J., N. Agrin, J. Leszyk, and G.B. Witman. 2005. Proteomic analysis of a eukaryotic cilium. *J. Cell Biol.* 170:103–113.

Rout, M.P., J.D. Aitchison, A. Suprapto, K. Hjertaas, Y. Zhao, and B.T. Chait. 2000. The yeast nuclear pore complex: composition, architecture, and transport mechanism. *J. Cell Biol*. 148:635–651.

Salisbury, J.L., A. Baron, B. Surek, and M. Melkonian. 1984. Striated flagellar roots: isolation and partial characterization of a calcium-modulated contractile organelle. *J. Cell Biol.* 99:962–970.

Sapiro, R., I. Kostetskii, P. Olds-Clarke, G.L. Gerton, G.L. Radice, and I.J. Strauss. 2002. Male infertility, impaired sperm motility, and hydrocephalus in mice deficient in sperm-associated antigen 6. *Mol. Cell. Biol.* 22:6298–6305.

Shang, Y., B. Li, and M.A. Gorovsky. 2002. *Tetrahymena thermophila* contains a conventional γ-tubulin that is differentially required for the maintenance of different microtubule-organizing centers. *J. Cell Biol.* 158:1195–1206.

Smith, D.S., M. Niethammer, R. Ayala, Y. Zhou, M.J. Gambello, A. Wynshaw-Boris, and L.H. Tsai. 2000. Regulation of cytoplasmic dynein behaviour and microtubule organization by mammalian Lis1. *Nat. Cell Biol.* 2:767–775.

Smith, J.C., J.G. Northey, J. Garg, R.E. Pearlman, and K.W. Siu. 2005. Robust method for proteome analysis by MS/MS using an entire translated genome: demonstration on the ciliome of *Tetrahymena thermophila*. *J. Proteome Res.* 4:909–919.

Stemm-Wolf, A.J., G. Morgan, T.H. Giddings Jr., E.A. White, R. Marchione, H.B. McDonald, and M. Winey. 2005. Basal body duplication and maintenance require one member of the *Tetrahymena thermophila* centrin gene family. *Mol. Biol. Cell*. 16:3606–3619.

Stolc, V., M.P. Samanta, W. Tongprasit, and W.F. Marshall. 2005. Genome-wide transcriptional analysis of flagellar regeneration in *Chlamydomonas reinhardtii* identifies orthologs of ciliary disease genes. *Proc. Natl. Acad. Sci. USA*. 102:3703–3707.

Tabb, D.L., W.H. McDonald, and J.R. Yates III. 2002. DTASelect and Contrast: tools for assembling and comparing protein identifications from shotgun proteomics. *J. Proteome Res.* 1:21–26.

Washburn, M.P., D. Wolters, and J.R. Yates III. 2001. Large-scale analysis of the yeast proteome by multidimensional protein identification technology. *Nat. Biotechnol.* 19:242–247.

Westermann, S., D.G. Drubin, and G. Barnes. 2007. Structures and functions of yeast kinetochore complexes. *Annu. Rev. Biochem.* 76:563–591.

Williams, N.E., C.-C. Tsao, J. Bowen, G.L. Hehman, R.J. Williams, and J. Frankel. 2006. The actin gene *ACT1* is required for phagocytosis, motility, and cell separation of *Tetrahymena thermophila*. *Eukaryot. Cell*. 5:555–567.

Wolfe, J. 1970. Structural analysis of basal bodies of the isolated oral apparatus of *Tetrahymena pyriformis*. *J. Cell Sci.* 6:679–700.

Wu, C.C., M.J. MacCoss, K.E. Howell, and J.R. Yates III. 2003. A method for the comprehensive proteomic analysis of membrane proteins. *Nat. Biotechnol.* 21:532–538.